

Lasers in Manufacturing Conference 2019

Laser powder bed fusion of pure copper using ultrashort laser pulses

Lisa Kaden^{a,*}, Gabor Matthäus^a, Tobias Ullsperger^a, Brian Seyfarth^{a,b}, Stefan Nolte^{a,b}

^a*Institute of Applied Physics, Abbe Center of Photonics, Friedrich-Schiller-Universität Jena, Albert-Einstein-Str. 15, 07745 Jena, Germany*

^b*Fraunhofer Institute for Applied Optics and Precision Engineering IOF, Albert-Einstein-Str. 7, 07745 Jena, Germany*

Abstract

One approach to broaden the range of available materials for additive manufacturing is the application of ultrashort laser pulses instead of using conventional cw or long-pulse lasers. The combination of high peak power and ultrashort interaction times allow the processing of materials exhibiting extraordinary high melting points, strong thermal conductivity or weak linear absorption. Also new materials based on hypereutectic alloys can be processed.

Here we present laser based powder bed fusion of pure copper parts using an ultrafast fiber laser system providing laser pulses with a duration of 500 fs at a wavelength of 515 nm. Typically pulse repetition rates in the MHz range are used in order to utilize heat accumulation effects. The additive manufacturing of sophisticated copper parts featuring microscopic resolution can be demonstrated. The produced samples are fully characterized in terms of surface quality, density, thermal and electrical conductivity. Moreover, the inner structure is revealed by X-ray computed tomography.

Keywords: additive manufacturing; 3D printing, laser based powder bed fusion; selective laser melting; ultrashort laser pulses; copper

1. Introduction

Laser based powder bed fusion (LPBF) also often called selective laser melting (SLM) evolved over the last two decades to the most important additive manufacturing technique for 3D printing of sophisticated metal parts. Numerous manufacturer provide a wide range of commercially available 3D printing machines capable to operate under normal industrial conditions. These machines are typically equipped with cw or long-pulse lasers featuring a wavelength either around 1030 nm (Ytterbium based systems) or 10.6 μm (CO_2 lasers). These systems are suitable for certain materials but cannot be applied for a wide range of materials [Santos et al., 2006]. In particular, hypereutectic alloys or materials with extraordinary properties like high transparency or

* Corresponding author. Tel.: +49 3641-947825; fax: +49 3641-947802.

E-mail address: lisa.kaden@uni-jena.de.

increased thermal conductivity cannot be processed [Nie et al., 2014, Ullsperger et al., 2017, Kaden et al. 2017].

A new approach is the application of ultrashort laser pulses. These lasers provide pulse durations below 100 ps (10^{-10} s). The corresponding peak power extends from MW to GW. As a consequence, the highest melting point of any material can be reached. As an example, the additive manufacturing of tungsten using ultrashort laser pulses was demonstrated [Nie et al., 2015]. The melting point of tungsten lies at around 3700 K. Also the processing of a hypereutectic aluminum silicon alloy was demonstrated. Here, the extraordinary short interaction times between laser radiation and matter allow to literally freeze the oversaturated melt pool at different metastable states exhibiting improved material properties [Ullsperger et al., 2017].

Recently, additive manufacturing of pure copper gained a lot of interest. However, additive manufacturing of pure copper turns out to be extremely challenging. Copper exhibits high thermal conductivity accompanied with high reflectivity at the near infrared [Joseph et al., 1998, Yoshida et al., 2004]. Moreover, at a processing wavelength around 1030 nm, the absorption coefficient reveals an abrupt increase at the transition from solid to liquid phase [Blom et al., 2003]. This particular characteristic makes it extremely difficult to proper control local melting. Previous publications discuss LPBF of pure copper using cw lasers [Pogson et al., 2003, Lykov et al., 2016]. Although the fabrication of dense copper parts with simplified geometries were demonstrated, no copper parts featuring complex geometries were shown. The final samples were also not characterized regarding final material characteristics like thermal or electrical conductivity.

In this paper we present additive manufacturing of sophisticated copper parts using ultrashort pulse laser radiation. The process is based on the powder bed fusion method. All samples were examined in order to measure the density and to reveal the inner structure. In particular, measurements using X-ray computed tomography were performed. Moreover, the electrical and thermal properties were studied.

2. Experimental setup

The setup was based on a self-constructed, computer controlled LPBF module in combination with an ultrafast fiber laser amplifier (Active Fiber Systems). The laser system delivered ultrashort laser pulses exhibiting a duration of 500 fs. In addition a second harmonic stage was installed in order to use a processing wavelength of 515 nm. An acousto-optic modulator (AOM) was applied to control the output power. The laser beam was finally guided through a galvanometer scanner and focused onto the building platform. By using a telescope, the final spot size was set to 30 μm ($1/e^2$). In order to prevent oxidation of the copper, LPBF was performed under nitrogen atmosphere. Here, the oxygen level was kept below 0.5 %. Within our experiments, copper powder with an average particle size of 10 μm (Alfa Aesar, purity ≥ 99 %) was used. Typically, layer thicknesses in the range between 15 - 30 μm were applied.

3. Results and discussion

As discussed in previous studies, the pulse repetition rate was set to 20 MHz, in order to exploit heat accumulation during laser melting [Kaden et al., 2017]. The processing wavelength of 515 nm was chosen due to the increased absorbance [Kaden et al., 2018]. Typically, pulse energies of around 1 μJ and scan velocities of several hundred mm/s were used. Using the processing parameters 3D printed copper featuring sophisticated geometries could be produced. Some examples are given in Fig. 1. The high degree of local resolution during processing is based on the confined heat affected zone during material processing using

ultrashort laser pulses. As a consequence, thin-wall structures exhibiting wall thicknesses below 100 could be fabricated (Fig. 1 a).

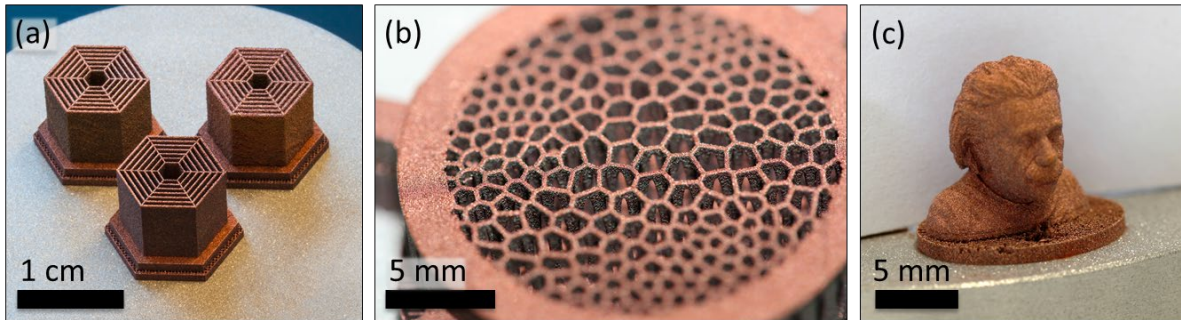


Fig. 1. (a) Thin wall samples with a minimum wall-thickness of 100 μm . (b) Mechanically optimized inner structure of a light-weight structure. (c) Miniature bust of Albert Einstein.

3.1. Density and inner structure

In order to investigate the density, cylindrical and cubic parts were fabricated. Using these samples, the volume and overall mass was measured. Typically, a density of 5.7 g/cm^3 is obtained. This corresponds to a filling factor of $\rho_{\text{rel}} = 64 \%$ compared to the bulk material. At the current state, this comparatively low value is due to limited average power provides by our laser system ($\approx 20 \text{ W @ } 515 \text{ nm}$). Although melting of a few copper grains can be observed, the extraordinary strong heat dissipation prevents the formation of a stable melt pool.

In addition, X-ray computed tomography (CT) was used to analyze the inner structure and density distribution. Here, cubic sample like the one shown in Fig. 2 a, were scanned with the help of a v|tome|x system from phoenix X-ray. This system used a voxel size of $5.4 \mu\text{m}$.

Fig. 2 c shows the cross-section perpendicular to the building direction. The image reveals a porous structure as expected from the density measurements. This analysis showed no significant differences between the cross sections perpendicular (Fig. 2 c) and parallel (Fig. 2 d) to the building direction. Hence, this implies an isotropic structure of the sample.

Observing the CT-data on a smaller scale points up a noisy signal (Fig. 2 e). Variations in the density below the voxel resolution and limitations in the X-ray computed tomography technology lead to the low signal-to-noise ratio. The applied X-ray power must be kept low to achieve a fine resolution, but this contradicts with the high X-ray absorption of copper. Therefore, a direct determination of the density through standard porosity analysis tools is not possible. By assuming the measured filling factor of the sample, a threshold to the grayscale data can be derived, so that the resulting binary data contains that filling factor. A cross-sectional image through the binary data is shown in Fig. 2 f. It is found that the copper samples have voids with dimensions of a few to $100 \mu\text{m}$, which are sometimes connected and form bigger cavities.

3.2. Electrical and thermal conductivity

The electrical conductivity was characterized using the van der Pauw method [Van der Pauw, 1958]. Our measurements revealed that the electrical conductivity of our samples was 6 Sm/mm^2 , which is one order of

magnitude lower than the value of pure copper given from literature $\sigma_{Cu} = 58.5 \text{ Sm/mm}^2$ [Joseph et al., 1998, Kaden et al., 2019].

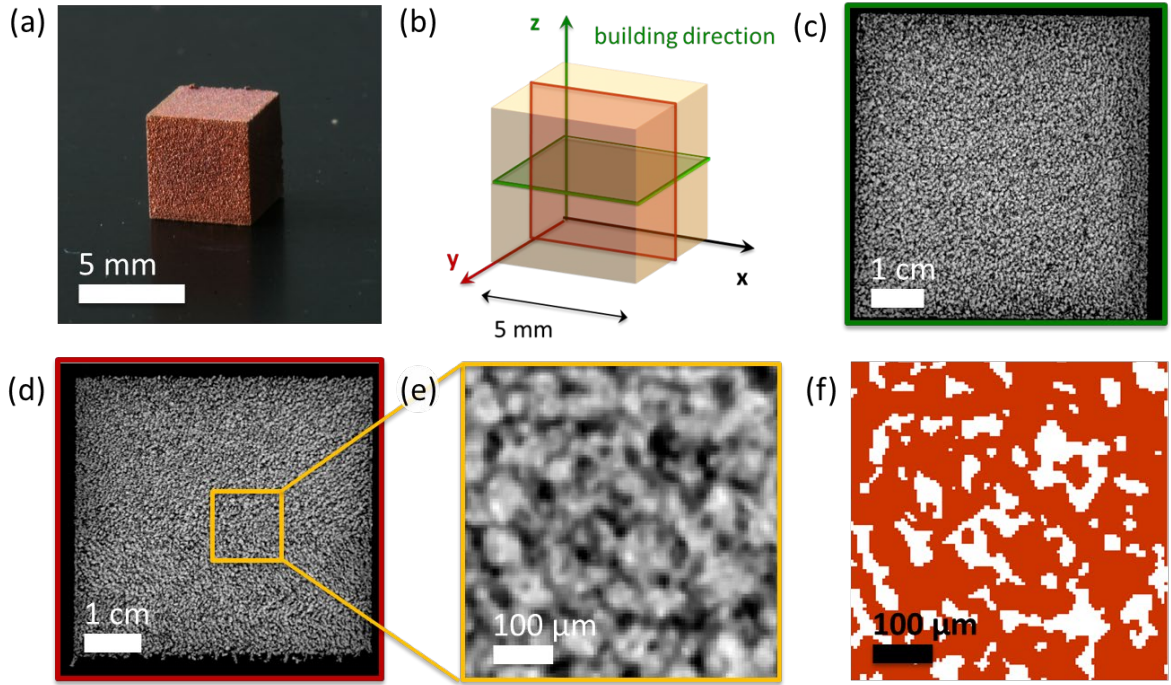


Fig. 2. (a) Cubic sample analyzed by X-ray computed tomography. CT-image of the cross section perpendicular (c) and parallel (d) to the building direction as shown in (b). (f) Using the measured filling factor, a monochrome image can be derived from the CT volume data given in (e). Hence, voids become visible and can be easily characterized.

The thermal diffusivity was measured using the light flash method. In our experiments a Netzsch LFA 447 Nano Flash was used. During this measurement, cylindrical samples were irradiated by a light flash and the temperature evolution on the rear side was recorded. From this temperature evolution, the thermal diffusivity through the sample were determined using the Cape-Lehman-model [Cape and Lehman, 1963]. Our measurements revealed that the diffusivity is around $30 \text{ mm}^2/\text{s}$, which corresponds to roughly 25% of the literature value for copper ($a_{Cu} = 114 \text{ mm}^2/\text{s}$ [Parker et al., 1961]). During our measurements we could not determine any differences of the thermal diffusivity parallel or perpendicular to the building direction. This supports the isotropic density distribution observed by CT measurements. Using the density together with the heat capacity, the thermal conductivity can be calculated using the following equation: $k = a \cdot c_p \cdot \rho$.

In this calculation we assume, that the underlying heat capacity is given by $c_p = \rho \cdot c_{p,Cu}$ with $c_{p,Cu} = 385 \text{ J/(kg K)}$ [Joseph et al., 1998]. Using this approach, a thermal conductivity $k_{\text{sample}} = 43 \text{ W/(mK)}$ was obtained. The literature value for copper is $k_{Cu} = 398 \text{ W/(m K)}$ [Joseph et al., 1998]. As a consequence, the same relation in comparison to the electrical conductivity can be derived, which is based on the fact, that the heat conduction in metals is mainly characterized by the electron system.

4. Conclusion

We demonstrated 3D printing of pure copper parts featuring highly sophisticated geometries. The process is based on the powder bed fusion method. As laser source, an ultrafast fiber laser system delivering 500 fs pulses at a wavelength of 515 nm was used. The 3D printed parts were characterized with respect to the inner structure, the electrical conductivity and the thermal properties. The average density was measured to be in the range of 5.7 g/cm^3 . Currently, this comparatively low value is due to the limited average power of our laser system (20 W). Although complete melting of single copper grains can be observed (instead of surface sintering), the extraordinary strong heat dissipation of pure copper prevents the formation of an extended melt pool. These results could be also verified by X-ray computed tomography of the printed parts, which revealed an isotropic but porous inner structure. Due to this morphology, the overall thermal and electrical conductivity was determined to be in the range of $\approx 1/10$ compared to the value of copper bulk material.

These results demonstrate that the density of the printed copper parts has serious impact on the electrical and thermal conductivity. In order to improve these values, a denser microstructure must be generated. In future experiments we will approach this issue by the application of increased average power during the LBPf process.

Acknowledgements

We like to acknowledge support from the German Federal Ministry of Education and Research (BMBF) within the project AM-OPTICS (02P15B203). Lisa Kaden was supported by TRUMPF Laser GmbH.

References

- Blom et al., 2003, Process spread reduction of laser microspot welding of thin copper parts using real-time control", Proc. SPIE 4977.
- Cape et al., 1963, Temperature and Finite Pulse-Time Effects in the Flash Method for Measuring Thermal Diffusivity, Journal of Applied Physics 34, p. 1909.
- Joseph et al., 1998, "Copper: Its Trade, Manufacture, Use and Environmental Status", ASM International, USA, p. 49.
- Santos et al., 2006, Rapid manufacturing of metal components by laser forming, Int. J. Mach. Tools Manuf. 46, p. 1459.
- Kaden et al., 2017, "Selective laser melting of copper using ultrashort laser pulses", Applied Physics A 123, p. 596.
- Kaden et al., 2018, Selective laser melting of copper using ultrashort laser pulses at different wavelengths, Proc. SPIE 1052312.
- Kaden et al., 2019, Additive manufacturing of pure copper using ultrashort laser pulses, Proc. SPIE 109090D.
- Lykov et al., 2016, Selective Laser Melting of Copper, Materials Science Forum 843 p. 284.
- Nie et al., 2014, Femtosecond laser melting and resolidifying of high-temperature powder materials", Appl. Phys. A 118, p. 37.
- Nie et al., 2015, Femtosecond laser additive manufacturing of iron and tungsten parts, Appl. Phys. A 119, p. 1075.
- Pogson et al., 2003, The production of copper parts using DMLR, Rapid Prototyp. J. 9, p. 334.
- Ullsperger et al., 2017, Selective laser melting of hypereutectic Al-Si40-powder using ultra-short laser pulses, Appl. Phys. A, 123, p. 798.
- van-der Pauw et al., 1958, A method of measuring specific resistivity and hall effect of discs of arbitrary shape, Philips Research Reports 13, p. 1.